Assessment of a drag-porosity approach in modeling urban-like turbulent flows

G.TIAN[a, b], B. CONAN[a, b], M. EI BAHLOULI [a] and I. CALMET[a, b]

a. Laboratoire de recherche en Hydrodynamique, Énergetique et Environnement Atmosphérique (LHEEA) - CNRS : UMR6598 - Ecole Centrale de Nantes - 1 rue de la Nöe 44321 BP 92101 Nantes Cedex 03, France

b. Institut de Recherche en Sciences et Techniques de la Ville - FR CNRS 2488 (IRSTV) - Ecole Centrale de Nantes - 1 rue de la Nöe 44321 BP 92101 Nantes, France

Résumé :

Ce travail présente l'analyse d'un écoulement turbulent au-dessus d'une canopée urbaine représentée par un agencement de cubes en quiconce. Deux modélisations numériques aux grandes échelles sont réalisées afin de comparer une approche utilisant des obstacles résolus avec une approche de type porosité-trainée. Des statistiques d'ordre élevé et un bilan de l'énergie cinétique turbulente sont analysés afin de caractériser l'écoulement, de comparer les approches et de se confronter à la littérature. Un des objectifs du travail est d'étudier les capacités et les limites de l'approche porosité-trainée pour la reproduction d'un l'écoulement instationnaire au-dessus d'une canopée urbaine.

Abstract :

This work presents the analysis of the turbulent characteristics developed over urban-like staggered cube arrays. The study proposes to use an obstacle-resolved and a drag-porosity large-eddy simulations. High order statistics and turbulent kinetic energy budget are analyzed for both approaches and compared to each other and to results from the literatures. One of the objectives is to evaluate the capacities and the limitations of a drag-porosity approach to reproduce unsteady turbulent flow over an urban canopy and to evaluate in details its performance.

Mots clefs : turbulent flow, Large eddy simulation, turbulent kinetic energy budget, OpenFOAM, urban canopy.

1 Introduction

The urban environment and citizen's living quality are strongly affected by human activities and urban morphology. Despite increasing computational power and more accurate measurement tools deepen the understanding of atmospheric turbulence, atmospheric turbulent flow mechanisms involved in urban areas are still very complex and remain an important scientific challenge. Dynamic properties of urban flows are studied in literature using numerical simulations such as direct numerical simulations

(DNS) and large-eddy simulations (LES) where the urban canopy is modeled by cubical obstacles arrays of varying density [1, 2, 3]. Although DNS resolves the Navier-Stokes equations without turbulence modeling it is only applicable to relatively low Reynolds number turbulent flow. LES resolves the large-scale motions of the flow and uses subgrid-scale (SGS) models to represent the effect of the small-scale turbulence.

For the study of real urban areas, the detailed knowledge of the buildings organization is unavailable and a drag-porosity approach may be preferable. The drag-porosity approach, as commonly used for forest canopies, models the presence of obstacles and their influence on the turbulent flow by a drag force that depends on averaged morphological characteristics of the canopy. It has the advantage of reducing the computation costs and can be applied for example to generate realistic inflow conditions for studies at the scale of some buildings. However, only few LES works exist on the use and efficiency of drag-porosity approach to represent the turbulent transfers between urban canopies and atmosphere [4, 5, 6]. The aim of the present study is to get insights on the main advantages and drawbacks of this approach by comparing results on turbulent statistics with those obtained in the same configuration when obstacles are explicitly accounted for.

In Section 2 the governing equations, the SGS model and the simulation configurations are presented. The results are discussed in section 3. Section 4 summarizes the major conclusions and draws perspectives of this work.

2 Governing equation and Numerical details

The filtered Navier-Stockes equations are written as follow:

$$\frac{\partial u_i}{\partial x_i} = 0 \tag{1}$$

$$\frac{\partial u_i}{\partial t} + \frac{\partial u_i u_j}{\partial x_j} = -\frac{1}{\rho}\frac{\partial p}{\partial x_i} + \nu\frac{\partial^2 u_i^2}{\partial x_j} - \frac{\partial \tau_{ij}}{\partial x_j} - f_i \tag{2}$$

In equations (1) and (2) the variables $\boldsymbol{u_i}$ and $\boldsymbol{p}$ represent the resolved-scale (filtered) velocity and pressure respectively, $\boldsymbol{\nu}$ is the fluid kinematic viscosity. The SGS stress tensor τ_{ij} is modeled following Smagorinsky [7] :

$$\tau_{ij} = -2\nu_{sgs}S_{ij} \tag{3}$$

where the resolved stain rate tensor is defined as:

$$S_{ij} = \frac{1}{2}\left(\frac{\partial u_i}{\partial x_j} + \frac{\partial u_j}{\partial x_i}\right) \tag{4}$$

and the SGS kinetic viscosity ν_{sgs} is modelled as:

$$\nu_{sgs} = {C_S}^2 \Delta^2 \sqrt{2S_{ij}S_{ij}} \tag{5}$$

The drag force f_i introduced in (2) to model the influence of the canopy in the drag-porosity approach is defined by:

$$f_i = \frac{1}{2}C_D(z)\alpha u_i\sqrt{u_k u_k} \tag{6}$$

where $C_D(z)$ is the drag coefficient profile extracted from obstacle-resolved simulation and α is the volumetric frontal density. In our configuration, $\alpha = 1/3h$, where h is the obstacle height. Note that $f_i = 0$ in the obstacle-resolved simulations.

The code is developed on the open source software $OpenFOAM2.4.0$, which uses finite volume method, combined with LES and standard Smagorisky SGS model [7] (equations (3)-(5)) with $C_S = 0.167$. Equations are solved using second-order implicit linear differencing for the spatial derivatives and second-order implicit linear backward differencing for the temporal integration. Figure 1 shows a plan view of the computational domain, with staggered cube arrays of dimensions $16h \times 12h \times 8h$. The finest grid used is $h/32$. Coceal [1] have confirmed that the simulations over cubic geometry are generally well resolved by $h/32$ mesh. Free-slip boundary condition is applied at the top of the domain. No-slip condition applied at the bottom and on all obstacle surfaces. Periodic boundary conditions are imposed both in spanwise and stream-wise directions to simulate an infinite array. The Reynolds number of the flow, based on the velocity at the top of the domain and the obstacle height is about 5000. The roughness Reynolds number R_τ based on the friction velocity u_* and obstacle height is about 500. To ensure the flow temporal convergence, simulations were run for an initial duration about $250T$, where $T = h/u_*$ is an eddy turnover time for the largest eddies shed by the cubes [1] . Statistics were collected and averaged over a further duration of $220T$ for computing flow statistics and turbulent kinetic energy budget.

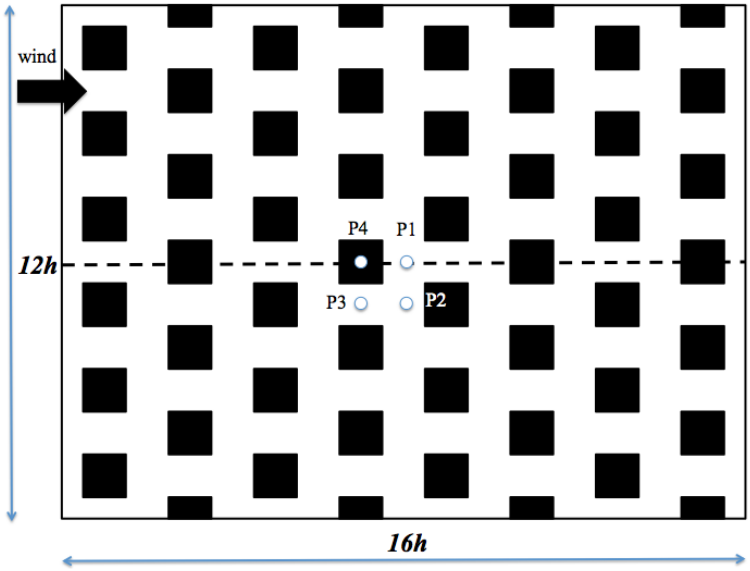

Figure 1. Plan view of the computational domain of the obstacle-resolved simulation

3 Results and discussion

3.1 Obstacle-resolved LES compared with DNS, LES and measurements from the literatures

In the following, $\boldsymbol{u}$, $\boldsymbol{v}$, $\boldsymbol{w}$ denote the stream-wise, spanwise and vertical velocity components, respectively. The vertical profiles of the time-averaged stream-wise velocity $\overline{u}$ over four typical locations P_1, P_2, P_3 and P_4 (Figure 1), normalized by the friction velocity u_* are plotted in Figure 2 and compared to wind tunnel measurements [8], DNS data [1, 2] and LES data [3]. In the present study, u_* is computed from the average drag force acting on the cubes.

The computed profiles of obstacle-resolved LES are in satisfactory agreement compared to the results from wind tunnel experiment [8] both within and above the canopy. Note that besides a coarser mesh ($h/32$) the present LES results are in very good agreement compared to the DNS from Coceal [1] where a $h/64$ mesh is used and Coceal [2]. Mean velicity profiles are in good agreement compared to LES data from Xie et al. [3].

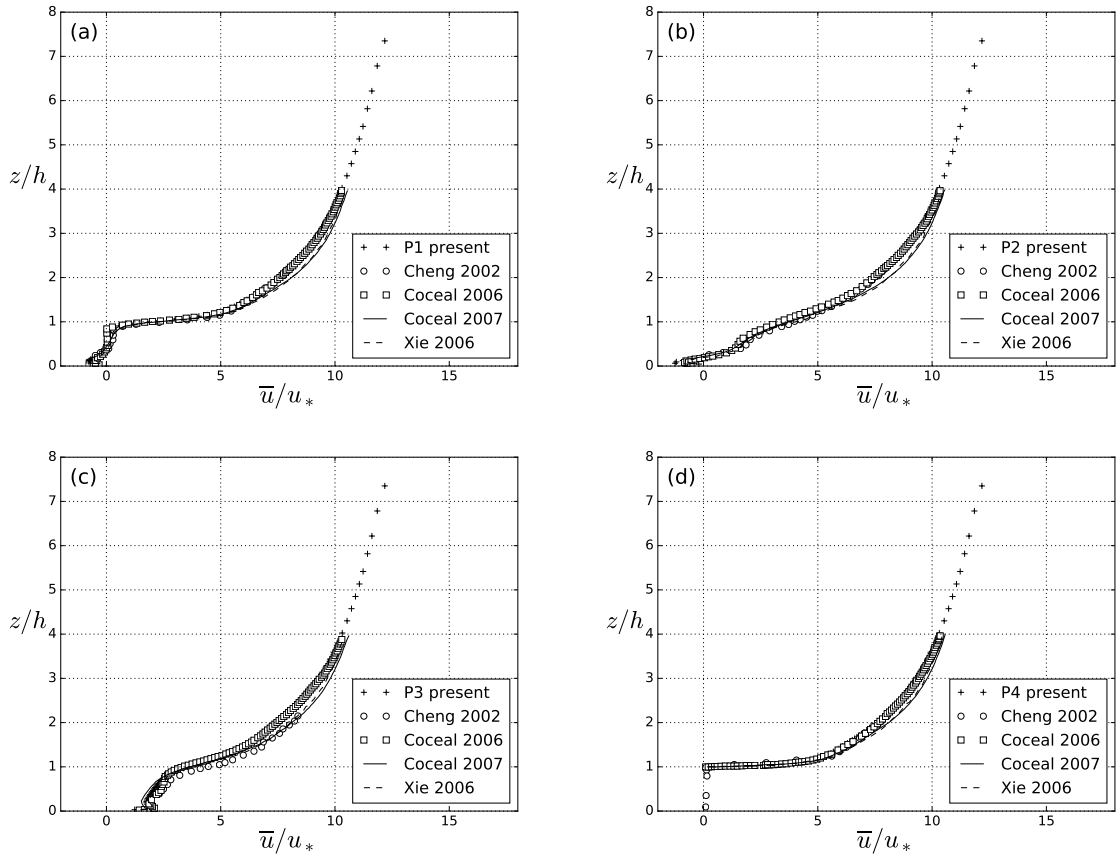

Figure 2. Vertical profiles of streamwise mean velocity $\overline{u}$ over four locations indicates in Figure 1.

Figure 3 presents the vertical profiles of the standard deviation of the longitudinal and vertical velocity components at positions P_1 (a, c) and P_2 (b, d) normalized by the friction velocity u_*. Compared to DNS data [2] and wind tunnel data [8], the present study gives good results above the canopy but always underestimates the velocity fluctuations inside. This is particularly the case for w_{rms} at P_2. Observations are in agreement to the observations of Coceal et al. [2] who found differences up to about 20%.

Figures 3 (e, f) present the Reynold shear stress $\overline{u'w'}$ profiles. Results show a good agreement compared to DNS data [2] and measurement data [8] both within and above the canopy. A peak at the height of $z = 0.1h$ is observed in the present LES results. This is was also observed in DNS results [1]. Following the argument of Xie et al. [3] this is presumably due to the resolution of a part of the boundary layer between two cubes.

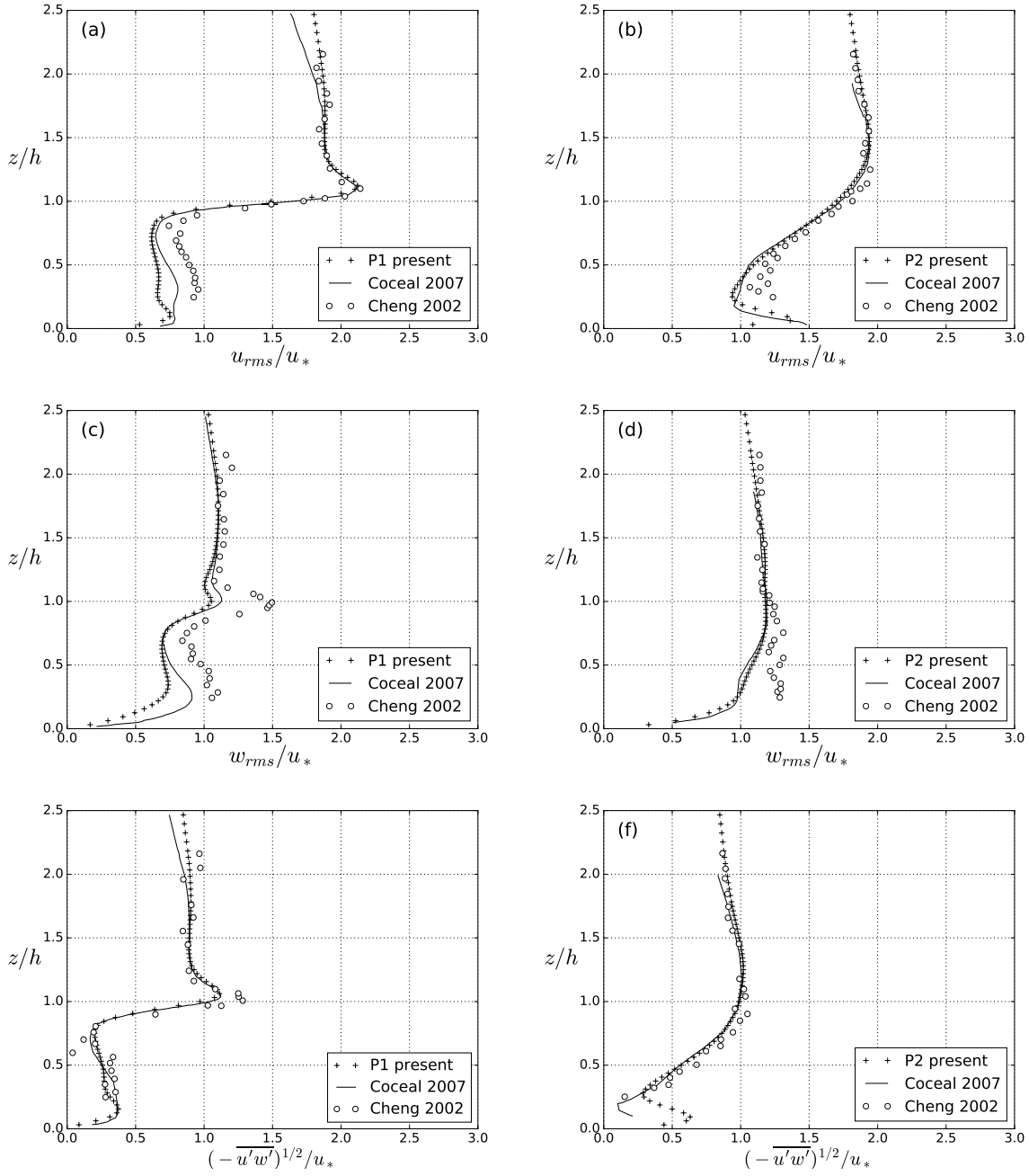

Figure 3. Vertical profiles of velocity standard deviation and Reynolds stress behind a cube at P_1 (a, c, e) and in front of a cube at P_2 (b, d, f)

3.2 Drag-porosity compared to obstacle-resolved approach

In this section, results from the drag-porosity simulation are presented and compared to the obstacle-resolved simulation. The drag coefficient used in the drag-porosity approach is calculated from the obstacle-resolved simulation by:

$$C_D(z) = 2\,\Delta p(z)/U^2(z) \tag{7}$$

where $\Delta p(z)$ is the mean of the laterally integrated pressure difference between the front and back faces of a cube and $U(z)$ is the spatially-averaged stream-wise mean velocity. Figure 4 shows the C_D

profile extracted from the present obstacle-resolved LES and from Maché [6] used in the drag-porosity approach and hereafter called "C_D-resolved" and "C_D-Mache", respectively. The "C_D-Mache" profile was optimized in order to model as closely as possible the mean velocity profile inside the canopy [6].

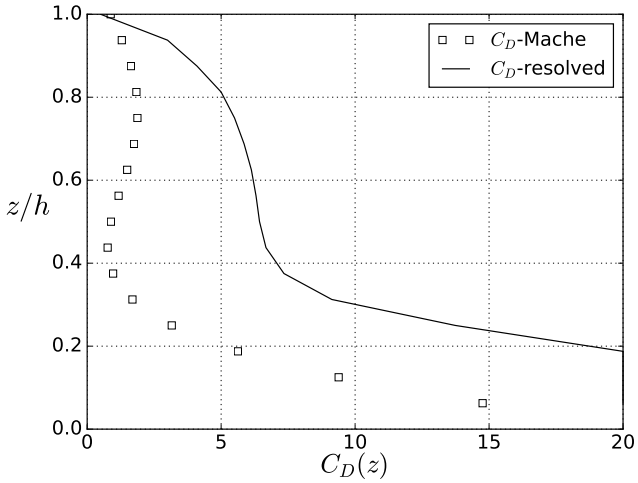

Figure 4. Vertical profile of drag coefficient C_D extracted from Maché [6] and from the obstacle-resolved LES.

The spatial and temporal stream-wise mean velocity $\overline{u}$ resulting from the drag-porosity LES performed with "C_D-Mache" and "C_D-resolved" (called "Porosity C_D-resolved", "Porosity C_D-Mache, respectively) are compared to obstacle-resolved LES in Figure 5. For all approaches, u_H is the mean velocity at $z = h$, u_* is calculated from the drag force: $u_* = \sqrt{\frac{F_D}{\rho A}}$ with F_D the drag force of a unit area and A the horizontal unit area. Mean profiles from the obstacle-resolved simulation are calculated using an horizontal space average, a discontinuity appears at $z = h$ because the average is performed only on fluid regions.

To assess the performance of the drag-porosity approach inside the canopy, Figure 5a shows the mean velocity profile normalized by the stream-wise mean velocity at $z = h$. In this graph, the C_D profile from Maché [6] fits the obatcle resolved profile better than another porosity result. On Figure 5b, the mean velocity profiles of both porosity approaches show a good agreement to the obstacle-resolved simulation above $z = h$, but different flow behavior inside the canopy. In gigure 5c, profiles are plotted in semilog axis and normalized by u_* from the drag force, d as the mean height of momentum absorption by the surface [2], and by z_0, the roughness length calulated from a log-law profile fitting. For $z > 1.5h$ results from the drag-porosity approach are in satisfactory agreement with the obstacle-resolved LES proving the reasonable choice of normalization for the upper flow. However, within the canopy, the drag-porosity approach seems to strongly reduce the mean velocity and deviate from the obstacle-resolved results.

Figure 5d shows that the Reynolds shear stress is better represented by the drag-porosity approach using "C_D-Mache" than using "C_D-resolved" profiles. The latter is overestimating the shear stress above the canopy and underestimating the shear stress inside the canopy.

Stream-wise and vertical standard deviation of the velocity, normalized by u_*, are shown in Figure 5e and Figure 5f. The drag-porosity simulation using "C_D-resolved" gives comparable u_{rms} profiles above the canopy whereas "C_D-Mache" leads to an underestimation. Below the canopy, both drag-porosity approches are under-estimating u_{rms}. This may be due to a too high drag force. For w_{rms}, using "C_D-

Mache" gives a good agreement above $z = h$ and "C_D-resolved" over-estimates the vertical turbulence intensity. Similarly to u_{rms}, inside the canopy, w_{rms} is too low for both approaches. The systematic over-estimation of turbulence above the canopy with the "C_D-resolved" may be the reason for a too high Reynolds shear stress (Figure 5d).

In general, the drag-porosity approach models reasonably well the air-flow above the canopy but results inside are poorer. The parametrized drag force coming from [6] gives the best fit inside the canopy.

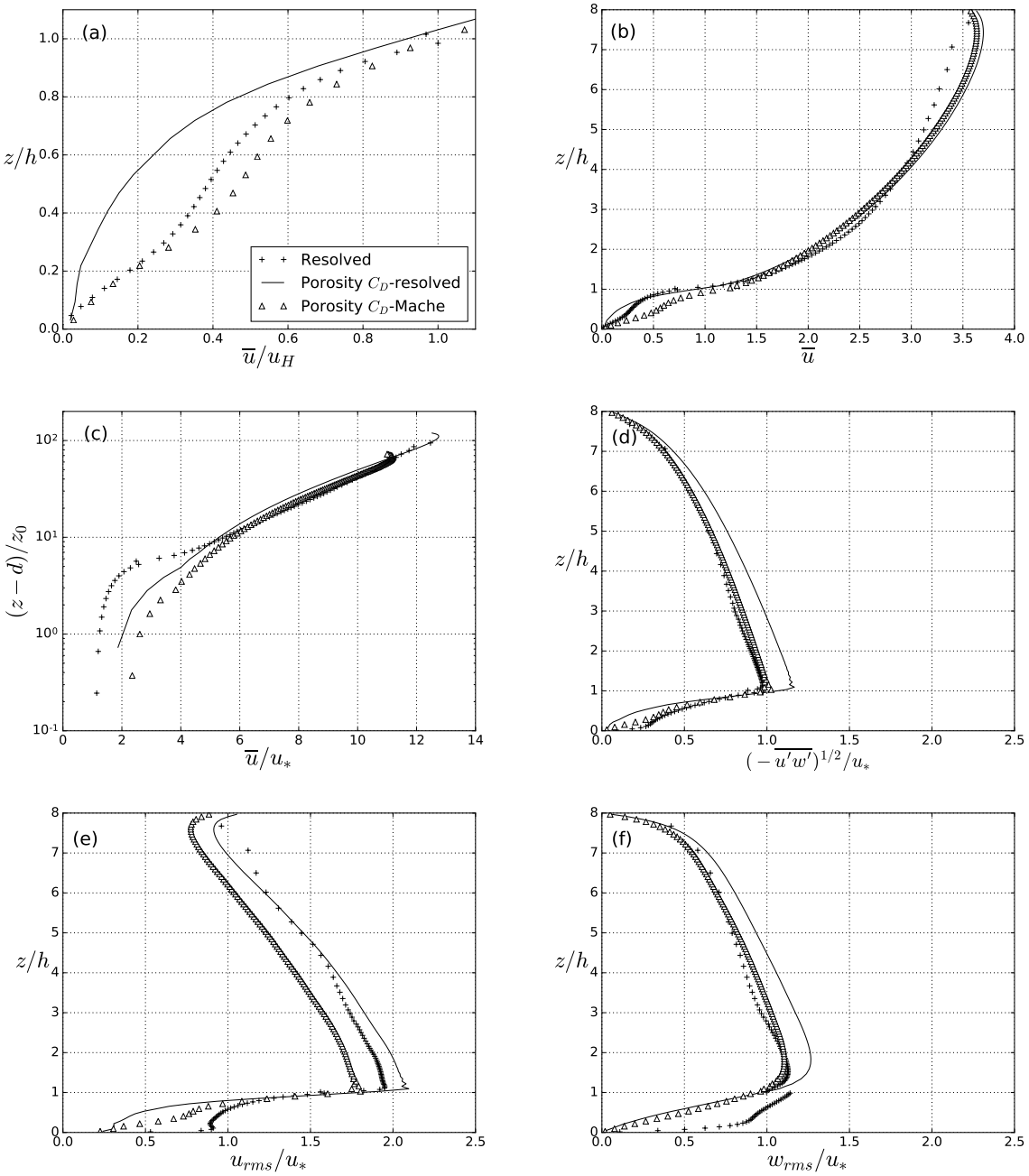

Figure 5. Vertical profiles of (a) spatial and temporal stream-wise mean velocity $\overline{u}$ within the canopy, normalized by u_H, (b) spatial and temporal stream-wise mean velocity $\overline{u}$, (c) Log law profile of $\overline{u}$, (d) spatial shear stress $\overline{u'w'}$, (e) spatial stream-wise turbulence intensities u_{rms}, (f) spatial vertical turbulence intensities w_{rms}, from (c) to (f) normalized by u_*, comparison between drag-porosity LES and obstacle-resolved LES.

3.3 Turbulent kinetic energy budget

To investigate further the energy transfers within and above the canopy, the turbulent kinetic energy (TKE) budget is computed [9, 10]. From the filtered Navier-Stokes equations (1)-(3) and assuming that the turbulent flow has reached a steady state, the TKE budget writes :

$$0 = \underbrace{-\overline{u_j}\frac{\partial}{\partial x_j}\frac{1}{2}\overline{u_i'u_i'}}_{A} \underbrace{-\overline{u_i'u_j'}\,\overline{S_{ij}}}_{P} \underbrace{-\frac{1}{2}\frac{\partial}{\partial x_j}\overline{u_i'u_i'u_j'}}_{T_r} \underbrace{-\frac{\partial}{\partial x_i}\overline{u_i'p'}}_{T_p} \underbrace{+\frac{\partial}{\partial x_j}2\nu\overline{u_i'S_{ij}'}}_{D_\nu} \underbrace{-2\nu\overline{S_{ij}'S_{ij}'}}_{\epsilon_r} \underbrace{-\frac{\partial}{\partial x_j}\overline{u_i'\tau_{ij}'}}_{T_{sgs}} \underbrace{+\overline{\tau_{ij}'S_{ij}'}}_{\epsilon_{sgs}} \tag{8}$$

where A represents advection by the mean flow, P is the production by shear, T_r is the transport by resolved velocity fluctuation, T_p is the transport by pressure fluctuation, D_ν is the viscous diffusion, ϵ_r is the resolved dissipation, T_{sgs} is the SGS transport, and ϵ_{sgs} is the SGS dissipation, which represents the transfer of energy from resolved to subgrid scales trough the cut-off. All these contributions to the TKE budget are directly computed from simulation results. Figure 6 shows these contributions for the obstacle-resolved simulation at two locations: P_1 in the wake of a cube, P_2 in the recirculation zone upstream of the cube.

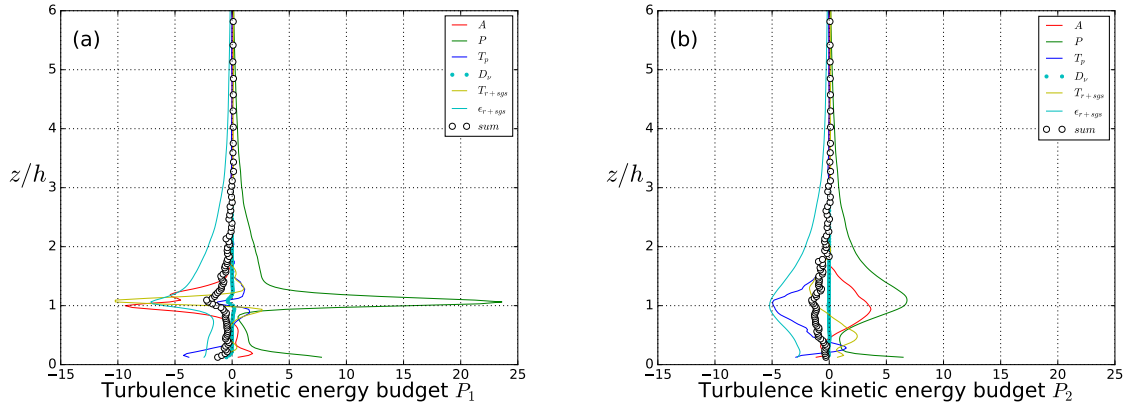

Figure 6. Vertical profiles of TKE budget terms, normalized by u_*^3/h, in obstacle-resolved LES for locations (a) P_1 and (b) P_2.

The TKE production reaches a maximum value just above the top of the canopy where the shear is the strongest (Figure 3). The maximum of Production decreases with the distance from the upstream cube while the shear layer becomes thicker. The Transport terms (T_r plus T_{sgs}) have negative value in the shear layer, but positive value below (at P_1 and P_2) and above (at P_1). It means that TKE is removed from this layer to be transferred downward and upward. The Transport by pressure fluctuations (T_p) acts in the same way as the transport by velocity fluctuations. However, this contribution is much more significant in front of a cube (at P_2) than behind (at P_1). The Advection term is also significant in the upper part of the canopy and in the shear layer. Depending on the location inside the wake or the recirculation it may be positive (at P_2) or negative (at P_1) and reverse sign in the lower part of the canopy. An analysis of the different terms contributing to the Advection in the upper part of the canopy shows that at P_1 (resp. P_2), the advection is linked with upward (resp. downward) mean flow.

As expected, above the roughness sublayer ($z/h > 2$), production and dissipation balance each other. In the vicinity of the canopy top, production and advection are compensated by transport and viscous dissipation at P_2 while the large production at P_1 is compensated by all other contributions. The balance is not exactly reached inside the roughness sublayer and a negative residual is observed (denoted sum on the figure). When the SGS contributions on transport and dissipation are omitted in the TKE budget (Figure 7), the residual becomes positive all over the domain height. The SGS transport is shown to have little influence on the total transport (expect in the thin shear layer at P_1). On the contrary, the SGS dissipation appears to be larger than the resolved dissipation. From these results, one can infer that the Smagorinsky model is well adapted to model SGS processes above the roughness sublayer but overestimate the TKE dissipation in regions where large instantaneous gradients occur.

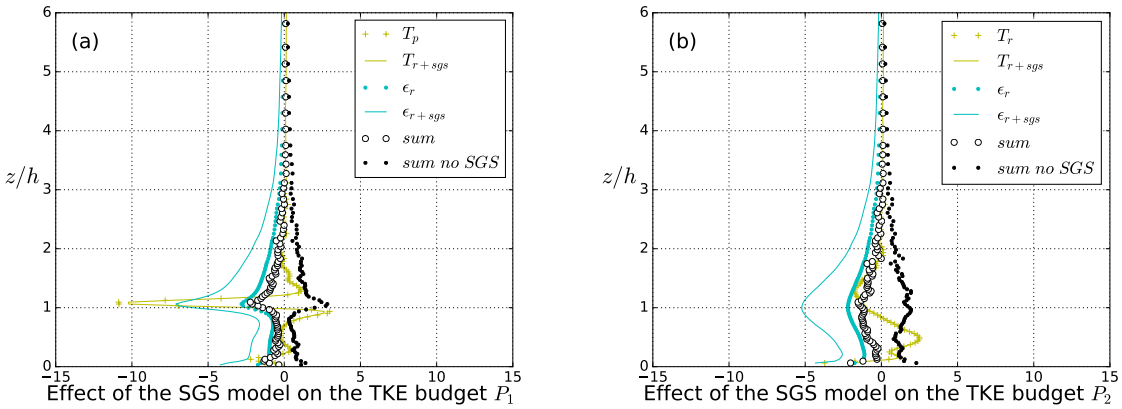

Figure 7. Effect of the SGS model on the TKE budget normalized by u_*^3/h in obstacle-resolved LES for locations,(a) P_1 and (b) P_2.

Figure 8 a and b present the spatially-averaged TKE budget(a) from the obstacle-resolved LES and (b) compared to the drag-porosity approach using "C_D-Maché". Figure 8 a differs from Figures 6 a and b as the production and dissipation balance down to $z = h$ with a rather sharp peak at that hight. The Advection term, of negative sign at $z = h$, shows the predominance of situations similar to P_1 where an upward flow is dominant. The pressure transport is, with the space-average, positive at $z = h$. Above $z = 2h$, both TKE budgets are presenting similar features with a balance between Production and Dissipation. Below $z = 2h$, Productions from both approaches are comparable, that suggests the drag-porosity approach succeeds well in reproducing TKE Production. On the other hand, the drag-porosity approach is completely underestimating Dissipation from $z = 2h$ down to the ground. This observation may be due to the poor reproduction of the shear layers developed on all sides of the cube, especially at $z = h$ and below, leading to a lack of small-scale structures dissipating TKE. Below $z = 1.5h$, the TKE budget is in large excess. Compared to the obstacle-resolved results, the Pressure transport term of the drag-porosity approach is reversed but the turbulent transport is rather similar. It can be also noticed that the Advection term is almost inexistent in the drag-porosity approach.

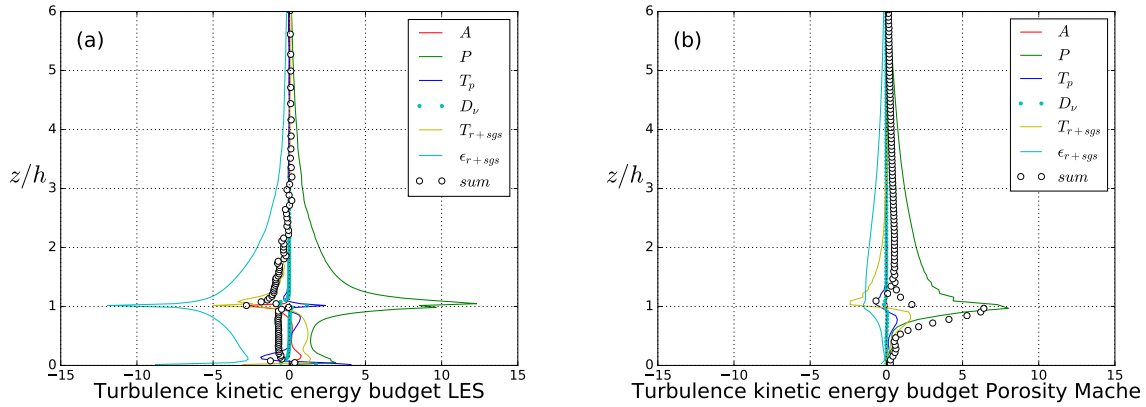

Figure 8. Vertical profiles of spatial averaged TKE budget normalized by u_*^3/h, (a) obstacle-resolved LES and (b) drag-porosity approach LES.

4 Conclusion

In sum, the obstacle-resolved LES over staggered cube arrays using Smagorinsky SGS model is in a very satisfactory agreement with both simulation data (DNS and LES) and measurement data from the literature. Based on the previous analysis, it confirmed that within the canopy, the mesh is fine enough to capture the detail of the flow, whereas above $z = 2h$, the coarser mesh is adapted and able to save computational cost.

The drag-porosity approach, tested for its limited computational cost, provided satisfactory results concerning the stream-wise mean velocity, the stream-wise and vertical turbulence intensities, and Reynolds shear stress above the canopy. However, developments are still needed to improve the performance of the drag-porosity approach to capture more detailed information, especially inside the canopy. The study also underlined the high influence of the drag coefficient profile.

TKE budgets are very different after a cube P_1 compared to before a cube P_2 especially concerning Advection, Turbulent transport and Pressure transport terms that are of invert sign. A peak of production is observed at P_1 due to the shear layer from the cube. Observations suggest that the SGS model is too dissipative for the obstacle-resolved simulation. The TKE budget of the drag-porosity approach leads to a correct representation above $z = 2h$ but differs from the obstacle-resolved simulation by the large lack of dissipation, the reversed sign of pressure transport and the almost null advection.

Observations made on mean velocity profiles, turbulence profiles and TKE budgets will be further analyzed to propose improvements to the drag-porosity approach.

Acknowledgment

This work was performed using the French national supercomputer facility Occigen from CINES and the supercomputer LIGER from Ecole Centrale Nantes. The first author gratefully acknowledge the financial support of the scholarship from China Scholarship Council (CSC) under the grant CSC N° 20158070084. The authors acknowledge the financial support of the French National Research Agency through the research grant URBANTURB N° ANR-14-CE22-0012-01.

References

[1] O. Coceal, T. G. Thomas, I. P. Castro, and S. E. Belcher, "Mean flow and turbulence statistics over groups of urban-like cubical obstacles," vol. 121, no. 3, pp. 491–519, 2006.

[2] O. Coceal, A. Dobre, T. G. Thomas, and S. E. Belcher, "Structure of turbulent flow over regular arrays of cubical roughness," vol. 589, 2007.

[3] Z. Xie and I. P. Castro, "LES and RANS for turbulent flow over arrays of wall-mounted obstacles," vol. 76, no. 3, pp. 291–312, 2006.

[4] T. Kono, T. Tamura, and Y. Ashie, "Numerical investigations of mean winds within canopies of regularly arrayed cubical buildings under neutral stability conditions," vol. 134, no. 1, pp. 131–155, 2010.

[5] S. Leonardi and I. P. Castro, "Channel flow over large cube roughness: a direct numerical simulation study," vol. 651, p. 519, 2010.

[6] M. Maché, *Représentation multi-échelle des transferts entre couche de canopée urbaine et atmosphère à l'échelle de la ville.* PhD thesis, Ecole Centrale de Nantes, 2012.

[7] J. Smagorinsky, "General circulation experiments with the primitive equations: I. the basic experiment," *Monthly weather review*, vol. 91, no. 3, pp. 99–164, 1963.

[8] H. Cheng and I. P. Castro, "Near wall flow over urban-like roughness," vol. 104, no. 2, pp. 229–259, 2002.

[9] W. Yue, C. Meneveau, M. B. Parlange, W. Zhu, H. S. Kang, and J. Katz, "Turbulent kinetic energy budgets in a model canopy: comparisons between LES and wind-tunnel experiments," vol. 8, no. 1, pp. 73–95, 2008.

[10] J. M. Tomas, M. J. B. M. Pourquie, and H. J. J. Jonker, "Stable stratification effects on flow and pollutant dispersion in boundary layers entering a generic urban environment," vol. 159, no. 2, pp. 221–239, 2016.